CrystEngComm

Accepted Manuscript

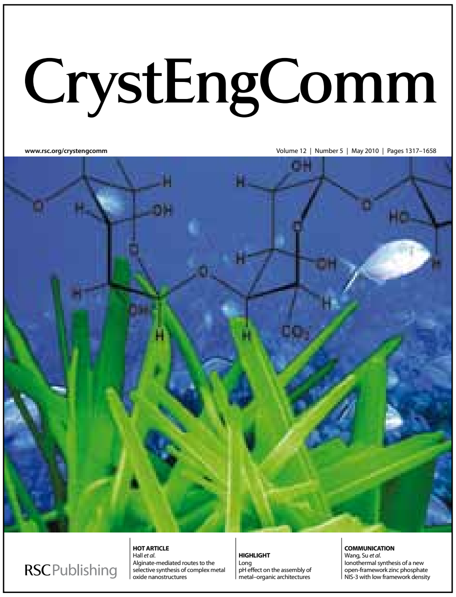
CrystEngComm

www.rsc.org/crystengcomm Volume 12 | Number 5 | May 2010 | Pages 1317–1658

RSC Publishing

HOT ARTICLE
Hall et al.
Alginate-mediated routes to the selective synthesis of complex metal oxide nanostructures

HIGHLIGHT
Long
pH effect on the assembly of metal–organic architectures

COMMUNICATION
Wang, Su et al.
Ionothermal synthesis of a new open-framework zinc phosphate NIS-3 with low framework density

This is an *Accepted Manuscript*, which has been through the RSC Publishing peer review process and has been accepted for publication.

Accepted Manuscripts are published online shortly after acceptance, which is prior to technical editing, formatting and proof reading. This free service from RSC Publishing allows authors to make their results available to the community, in citable form, before publication of the edited article. This *Accepted Manuscript* will be replaced by the edited and formatted *Advance Article* as soon as this is available.

To cite this manuscript please use its permanent Digital Object Identifier (DOI®), which is identical for all formats of publication.

More information about *Accepted Manuscripts* can be found in the **Information for Authors**.

Please note that technical editing may introduce minor changes to the text and/or graphics contained in the manuscript submitted by the author(s) which may alter content, and that the standard **Terms & Conditions** and the **ethical guidelines** that apply to the journal are still applicable. In no event shall the RSC be held responsible for any errors or omissions in these *Accepted Manuscript* manuscripts or any consequences arising from the use of any information contained in them.

RSC Publishing

www.rsc.org/crystengcomm

Registered Charity Number 207890

Silica/Ultrasmall Ag Composite Microspheres: Facile Synthesis, Characterization and Antibacterial and Catalytic Performance

Xin-Hui Liu[a,b], Yan-Yan Cao[a], Huang-Yong Peng[a], Hai-Sheng Qian*[,a], Xian-Zhu Yang[a], Hong-Bin Zhang*[,a]

[a] *Institute of Smart Biomedical Materials and Device, School of Medical Engineering, Hefei University of Technology, Hefei 230009, P. R. China.*

[b] *Department of Chemistry, College of Chemistry and Life Sciences, Zhejiang Normal University, Jinhua 321004, P. R. China.*

RECEIVED DATE (to be automatically inserted after your manuscript is accepted if required according to the journal that you are submitting your paper to)

*Corresponding author. E-mail: shqian@hfut.edu.cn (Prof. H.S. Qian), Fax: 0086 551 62901285, Fax: 0086 551 62901285

[a] School of Medical Engineering, Hefei University of Technology, Hefei 230009, P. R. China.

Abstract

Uniform silica/ultrasmall silver composite microspheres has been prepared from $[Ag(NH_3)_2]^+$ in presence of silica microspheres via a hydrothermal process. The reaction temperature plays a critical role in the formation of the as-prepared SiO_2/ultrasmall Ag composite microspheres. The as-prepared product was investigated by X-ray diffraction (XRD), field-emission scanning electron microscopy (FESEM, JEOL-6700F) and transmission electron microscopy (TEM, JEOL 3010), respectively. The silica/ultrasmall silver composite microspheres are with 200 nm in diameters and the silica microspheres decorated with ultrasmall Ag nanoparticles with an average diameter of 4 nm. As expected, the as-prepared silica/ultrasmall silver composite microspheres exhibit superior bacteriostatic and bactericidal activities and excellent photodecomposition toward Rhodamine 6G (R6G) dyes.

Key words: Silica Microspheres, Ultrasmall Ag Nanocrystals, Antibacterial Activities, Hydrothermal Synthesis

1. Introduction

Noble metal nanoparticles have attracted much interest because of their unique properties, including large optical field enhancements resulting in the strong scattering and absorption of light; which has been widely applied in optical and imaging fields, photothermal therapy and high electro-oxidation activity etc.[1,2] Over the past decade, many efforts have been paid to synthesize silver nanostructures with different size and morphologies including silver cubes,[3,4] nanoparticles,[5,6] nanorods[7,8] and nanowires.[9,10] Silver nanoparticles have found applications in catalysis, optics and electronics due to their unique size-dependent optical, electrical and magnetic properties.[11,12] Additionally, silver nanoparticles have been widely used in antibacterial/antifungal agents in biotechnology and bioengineering, textile engineering, water treatment to eliminate microorganisms.[13, 14] However, the silver nanoparticles with small size aggregate in media with a high electrolyte content, resulting in a loss of antibacterial activities because the antibacterial activities of silver nanoparticles are related to their size, with the smaller particles having higher activities on the basis of equivalent silver mass content.[15] Hence, Ag nanoparticles embedded into solid substrates can stabilize the silver nanoparticles against aggregation, leading to retention of the antibacterial activities.

In recent years, Ag-based composites including polystyrene microsphere/reduced grapheme oxide/Ag composites,[16] polyurethane/silver composite nanofibers,[17] silica/Ag,[18] carbon/Ag microspheres,[19,20] polystyrene/Ag microsphere,[21] polyamide/silver composites,[22] polyphosphazene /Ag nanotubes,[23] $TiO_2/SiO_2/Ag$ nanocomposites[24] and $Fe_3O_4/SiO_2/Ag$ nanospheres[25] have been achieved so far. In contrast to other matrix, silica occupies its unique advantages owing to its better chemical stability and biocompatibility. Many synthetic methods have been developed to synthesize silica/Ag composite microspheres. For examples, a two-step solution process has been developed to synthesize SiO_2/Ag composite spheres; which was fabricated from reducing of the $[Ag(NH_3)_2]^+$ ions adsorbed by silica microspheres using ethanol and PVP as reducing agents.[26] Ag nanoparticles with average sizes of

20 nm were well-dispersed on the surfaces of Fe_3O_4@SiO_2 composite microspheres through a simple wet-chemical method employing the Ag-mirror reaction.[24] Immobilization of silver nanoparticles onto silica spheres effectively protects metal particles from aggregation, thus avoiding deactivation and poisoning of the catalysts during the catalytic reaction and retention of the antibacterial activities. Nevertheless, these methods involved either surface functionalization of silica microspheres-a relatively long period of processing time or using of some reducing agents.

In this communication, a facile hydrothermal process has been successfully developed to synthesize uniform silica/ultrasmall silver composite microspheres using $[Ag(NH_3)_2]^+$ as starting materials in presence of silica microspheres. The silica/ultrasmall silver composite microspheres are with 200 nm in diameters and the silica microspheres decorated with ultrasmall Ag nanoparticles with an average diameter of 4 nm. The reaction temperature and reaction time play important role in the formation of the SiO_2/Ag composite microspheres. The as-prepared silica/ultrasmall silver composite microspheres exhibit superior and durable bacteriostatic, bactericidal and catalytic activities owing to the antimicrobial ability of the ultrasmall Ag nanoparticles embedded in silica microspheres.

2. Results and discussion

2.1 The synthesis and characterization of uniform silica/Ag microspheres

The first step of the synthesis of uniform silica/Ag microspheres involved the production of uniform silica microspheres with 200 nm in diameters via a modified protocol.[27,28] The scanning electron microscopy (SEM) and transmission electron microscopy (TEM) images have been shown in Fig. S1 (in the supporting information). Fig. 1 c shows X-rays diffraction pattern of the as-prepared sample obtained from reaction of 0.5 g silica microsphere and 1 mmol $[Ag(NH_3)_2]^+$ at 180 ^oC for 24 h; in which all of the peaks can be readily indexed to face centered-cubic silver (JCPDS No. 04-0718) a cell constant of a = 4.086 Å.[29,30] The morphologies of the as-prepared sample has been carried out using field emission scanning electron microscopy (FESEM) and transmission electron microscopy (TEM) analyses. Fig. 1a, b show SEM images of the as-prepared SiO_2/Ag microspheres with 200 nm in diameters; which is in accordance with the size of silica microspheres used as templates. The TEM images of the silica/Ag microspheres have been shown in Fig. 1d-e, illustrating the silica microspheres decorated with small aggregates of ultrasmall Ag nanoparticles with an average diameter of 4 nm.

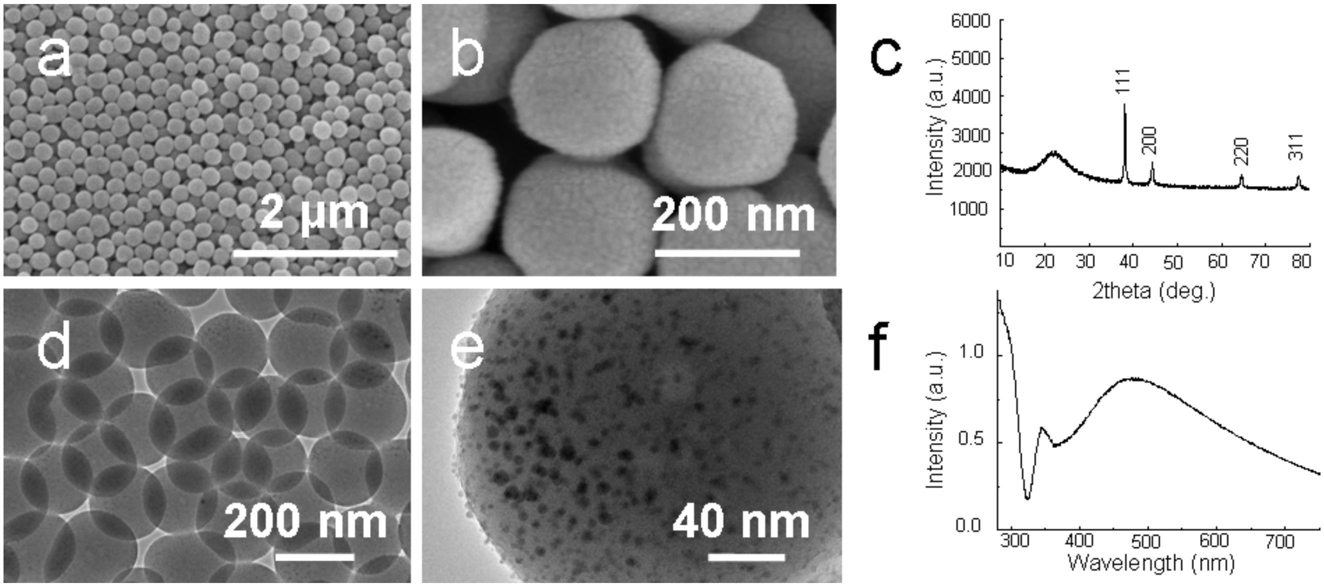

Fig. 1. (a-b) SEM images of the silica/Ag microspheres obtained from 1 mmol $[Ag(NH_3)_2]^+$ in presence of 0.5 g silica microspheres at 180 °C for 24 h; (c) XRD patterns of the silica/Ag microspheres; (d-e) TEM images of the silica/Ag microspheres; (f) UV-vis spectra of the silica/Ag microspheres.

In this work, the ultrasmall nanoparticles of Ag with several nanometers in diameters has been observed and stabilized by embedding into the silica microspheres. The optical absorption of the SiO_2/Ag microspheres has been characterized using UV-vis absorption spectra, which has been shown in Fig. 1f. There are two adsorption peaks located at 348 nm and 480 nm instead of the classical single peak corresponding to the plasmon resonance in spherical inclusions.[31] The peak located at 348 nm as shown in Fig. 1f could be derived from the surface plasmon resonance of ultrafine nanoparticles of silver, illustrating the silver nanoparticles with 4 nm in diameters owing to the plasmon resonance blue shifts when the nanoparticles' diameter decreases from 20 nanometers to less than two nanometers according to the previous study.[32] A wide absorption peak located at 480 nm range from 380 nm to 800 nm as shown in Fig. 1e could be attributed to the bigger size of the silver nanoparticles partially derived from the aggregation of silver nanoparticles during the growth process; which largely broadens the size and shape distribution illustrating the shift and width of the absorption peak.[33] However, the optical absorption of the as-prepared SiO_2/Ag microspheres was derived from the formed silver nanoparticles; which is depended on the concentration of $[Ag(NH_3)_2]^+$ and silica microspheres used in reactions. As shown in the Fig. S2, the UV-vis absorption spectra of the as-prepared SiO_2/Ag composite microspheres obtained from 0.5 mmol $[Ag(NH_3)_2]^+$ in presence of 0.5 g silica microspheres at 180 ^oC for 24 hour indicated that the silver nanoparticles with 4 nm in diameters were well dispersed in silica microspheres; which also revealed by the TEM images (in the supporting information Fig. S3). The X-ray photoelectron spectra (XPS) of the SiO_2/Ag composite spheres obtained from 1 mmol $[Ag(NH_3)_2]^+$ in presence of 0.5 g silica microspheres at 180 ^oC for 24 h were measured to examine the composition of the surface, as shown in Fig. 2. Peak values at 284.8, 532.9 and 103.7 eV can be readily assigned to the binding energies of C1s, O1s and Si2p, respectively. The peak with binding energy at 368.7 and 374.6 eV for Ag3d can be assigned to the Ag 3d5/2 and Ag 3d3/2, respectively.[34] In addition, the Ag 3d5 peak centered at 368.7eV is readily assigned to Ag^0 according to the previous studies.[35,36] On the base of the XPS analyses, the element composition of the as-prepared SiO_2/Ag microspheres were also listed in Table S1 (in supporting information) illustrating the atomic percent of Ag is 0.3 %.

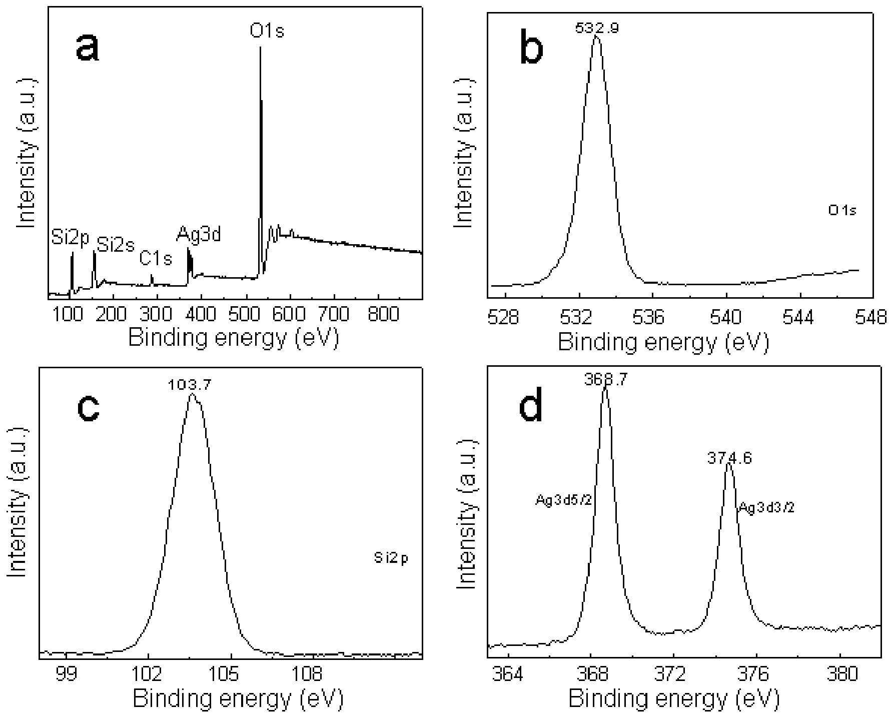

Fig. 2. XPS spectra of the SiO_2/Ag composite spheres obtained from 1 mmol $[Ag(NH_3)_2]^+$ in presence of 0.5 g silica microspheres at 180 ^oC for 24 h. (a) Survey spectrum; (b) O1s; (c) Si2p; (d) Ag 3d.

Several experimental observations have been helped to illustrate the formation process for SiO_2/ultrasmall Ag composite microspheres. In the present study, the temperature plays a critical role in the formation of the as-prepared SiO_2/ultrasmall Ag composite microspheres. No cubic phase Ag was observed when the reaction occurred at 140 ^{o}C as XRD patterns revealed by Fig. S4a. When the reaction temperature was raised to 160 ^{o}C, weak peaks located at 37.8 , 44.2, 64.5, and 77.5 ^{o} have been clearly observed, which could be indexed to the diffraction of the 111, 200, 220 and 311 crystal planes of cubic silver (in the supporting information Fig. S 4b). In general, an increase in temperature is accompanied by an increase in the reaction rate. As we have observed here, the whole process may be described by the following reactions.

$$[Ag(NH_3)_2]^+ \Leftrightarrow Ag^+ + 2NH_3 \qquad (1)$$

$$NH_3 + SiO_2 \rightarrow NH_4^+ + SiO_3^{2-} \qquad (2)$$

$$2\mathrm{Ag}^+ + 2\mathrm{OH}^- \rightarrow \mathrm{Ag_2O} + \mathrm{H_2O} \rightarrow \mathrm{Ag} + \mathrm{O_2} \qquad (3)$$

When the temperature was raised to (or higher than) 160 ^{o}C, the reaction (2) rate would be increased greatly and the excessive NH_3 solution would be consumed resulting into formation of silver nanoparticles as illustrated in the reaction 2 and 3. In present study, the silica microspheres would be etched resulting into formation SiO_2/ultrasmall Ag composite microspheres with porous nanostructures according to the previous study revealed by the Prof. Yin et al.[37,38] The N_2 adsorption-desorption isotherm shown in Fig. S5 (in the supporting information) illustrated that the SiO_2/ultrasmall Ag composite microspheres are with higher Brunauer-Emmett-Teller (BET) specific surface area (ca. 18.5 $m^2.g^{-1}$) compared to the silica microspheres (ca. 1.0 $m^2.g^{-1}$). To gain a better understanding on the growth mechanism of these uniform SiO_2/ultrasmall Ag composite microspheres, the products formed at early stages were collected for UV-vis spectra and XRD analysis. Fig. 3A shows the UV-vis absorption spectra of the as-prepared samples at 180 ^{o}C for different time; which indicates that the peaks located at around 348 nm and 480 nm increased gradually due to formation and growth of silver nanoparticles formed at the first stage and also revealed and testified by XRD patterns shown in Fig. 3B.

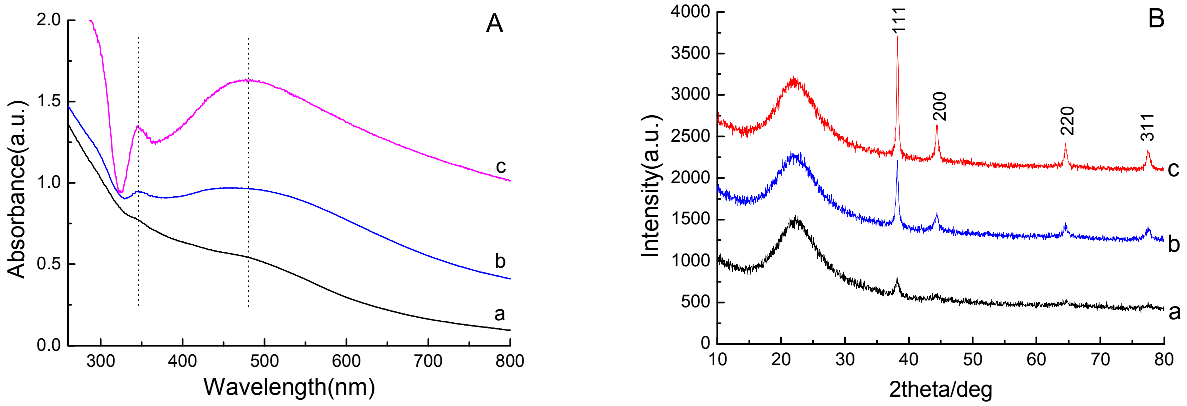

Fig. 3. UV-vis absorption spectra (A) and XRD patterns (B) of the as-prepared SiO_2/Ag composite microspheres at 180 °C for 4 h (a); (b) 6 h and 12 h (c); respectively.

2.2 The antibacterial properties of uniform silica/Ag microspheres

Ag nanoparticles demonstrated a unique antimicrobial property against multidrug-resistant bacteria, based on its capability of generating the intracellular reactive oxygen species (ROS). [39,40] Herein, Escherichia Coli (E. Coli) was chosen as a bacterial model and incubated in presence of as-prepared SiO_2/Ag microspheres with different concentration and followed by OD_{600} measurements to evaluate bacterial growth. Fig. 4 shows that the antimicrobial activities of the as-prepared SiO_2/Ag microspheres against E. Coli, indicating the product obtained from 0.25 g silica microsphere and 1 mmol $[Ag(NH_3)_2]^+$ at 180 °C for 24 h showing more superior antimicrobial performance. The minimal inhibitory concentrations (MICs) and minimum bactericidal concentrations (MBCs), adopted to quantitative analysis the bacteriostatic and bactericidal properties of the samples against pathogenic organisms are summarized in Table S2 (in the supporting information). The as-prepared SiO_2/Ag microspheres exhibited superior bacteriostatic and bactericidal activities owing to the antimicrobial ability of the Ag nanoparticles embedded in silica microspheres. In other word, as shown in Table S2 (in the supporting information), the SiO_2 microspheres decorated with the highest population of Ag nanoparticles would have the lowest minimal inhibitory concentrations (MICs) and minimum bactericidal concentrations (MBCs); which is in good accordance with the reactions mechanism discussed in the previous section. In addition, the silica microspheres show good biocompatible and no antimicrobial property even when the concentration of the silica microspheres is up to 500 μg/L.[28] The antibacterial activities of silver nanoparticles are related to their size and with high populations of Ag, with the smaller particles having higher activities owing to their ultra-high surface to volume ratio and unique surface chemistry compared with their larger counterparts.[41] In general, the silver nanoparticles with several nanometers in diameters aggregate in media with high electrolyte content, resulting in a loss of antibacterial activities. As expected, the SiO_2/Ag microspheres have superior antibacterial activities owing to silver nanoparticles embedded into the microspheres of silica, resulting into preventing the aggregation of silver nanoparticles. In particular, the antibacterial activities of the SiO_2/Ag microspheres are dependent on chemisorbed Ag^+, which is readily formed owing to extreme sensitivity to oxygen for the ultrasmall Ag nanoparticles.

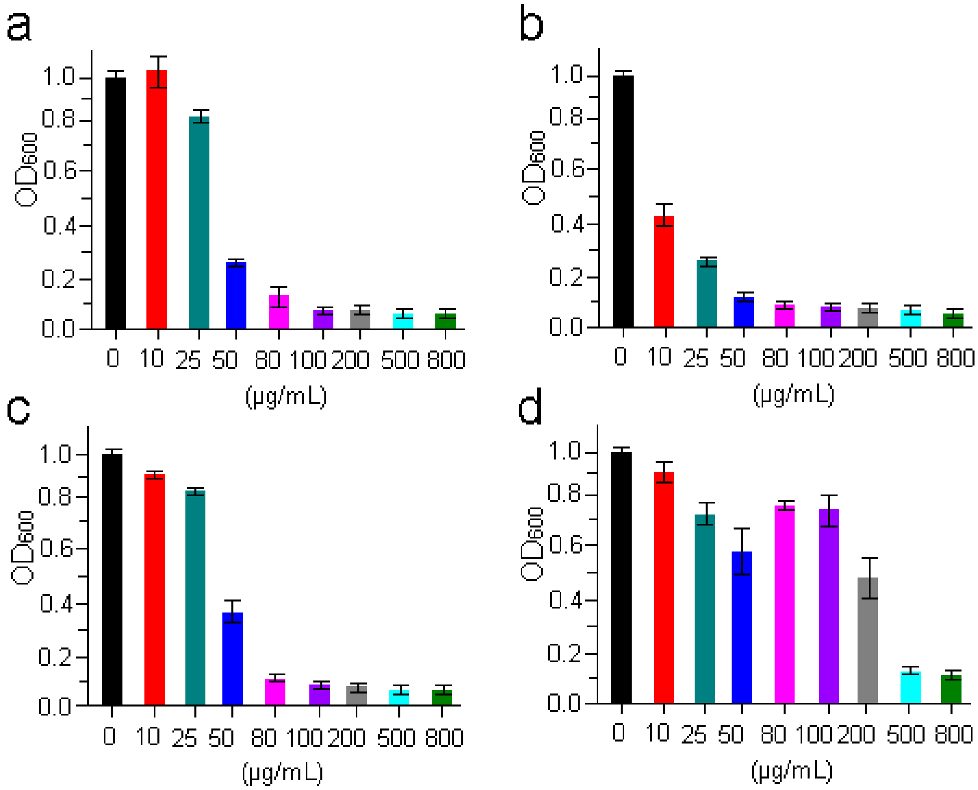

Fig. 4. The growth inhibition of E. Coli strains in presence of the as-prepared SiO_2/Ag microspheres obtained from different condition. (a) 0.5 g silica microsphere and 1 mmol $[Ag(NH_3)_2]^+$ at 180 °C for 24 h; (b) 0.25 g silica microsphere and 1 mmol $[Ag(NH_3)_2]^+$ at 180 °C for 24 h; (c) 0.25 g silica microsphere and 1 mmol $[Ag(NH_3)_2]^+$ at 160 °C for 24 h; (d) 0.5 g silica microsphere and 0.5 mmol $[Ag(NH_3)_2]^+$ at 160 °C for 24 h. The data are expressed as mean standard deviation of three replicates.

Standard deviation is indicated by the error bars.

2.3 The photocatalytic performance of SiO_2/Ag microspheres.

Herein, the photodecomposition of Rhodamine 6G (R6G) was chosen as a model reaction to examine the catalytic properties of SiO_2/Ag hybrid microspheres. The characterized peak located at 526 nm for R6G solution measured by a UV-vis spectrophotometer was used to determine its reduction efficiency at given time interval. Fig. 5a show that nearly 100 % of R6G have been photodegraded within 5 min under visible light irradiation using a 250 W Xe lamp indicating the as-prepared SiO_2/Ag hybrid microspheres with excellent catalytic performance towards the R6G solution. In addition, as shown in Fig. 5b, the photodecomposition of Rhodamine R6G drops only slightly in the four successive cycles and rapidly in fifth cycle primarily because the Ag catalysts over the surface of silica microsphere unprotected by the silica substrate.

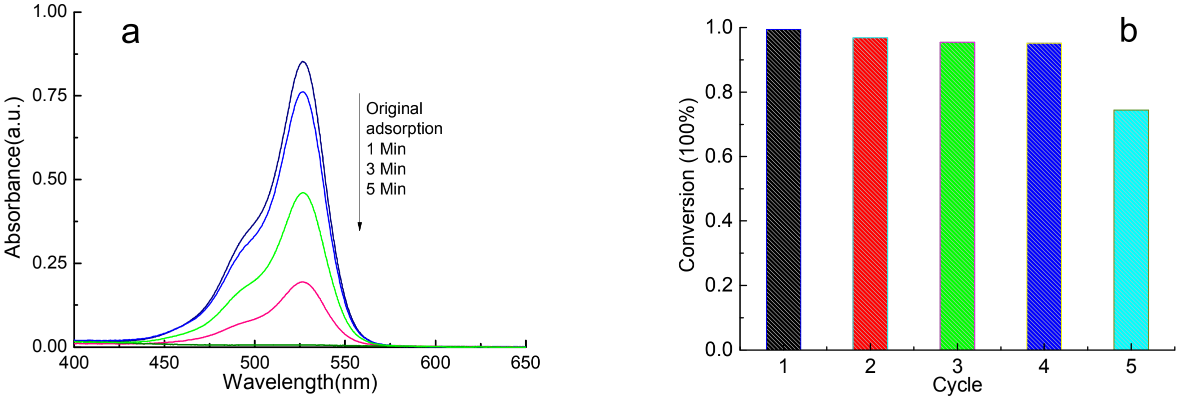

Fig. 5. (a) Time dependent absorption spectra for the catalytic reduction of R6G by $NaBH_4$ in the presence of the as-prepared SiO_2@Ag nanospheres; (b) plot of conversion of R6G in five successive cycles using the as-prepared SiO_2@Ag nanospheres with the same irradiation time.

3. Experimental

Chemicals. Tetraethyl orthosilicate (TEOS, >99.5 wt %), silver nitrate ($AgNO_3$, > 99.8 wt %), ammonia solution (25-28 wt %) and ethanol were purchased from Shanghai Chemical Ltd. All chemicals are of chemical grade and used without purification further.

3.1 The synthesis of amorphous silica microspheres with 200 nm in diameters. In a typical process, 1 mL tetraethyl orthosilicate (TEOS) was dissolved with 20 mL ethanol to form clear solution with vigorous stirring; and then 3 mL ammonia solution (25-28 wt %) was added by dropwise into the previous solution and aged at room temperature for 24 h. the product in white (the amorphous silica nanospheres) was collected by centrifugation and washed several times with absolute ethanol, and finally dried at 60 °C for 4 h.

3.2 The synthesis of SiO_2/ultrasmall Ag composite microspheres. The uniform SiO_2/ultrasmall Ag composite microspheres has been obtained from reaction of silica microspheres and $[Ag(NH_3)_2]^+$ solution by hydrothermal process. In a typical procedure, 1 mmol $AgNO_3$ was dissolved with 22 mL double distilled water to form clear solution, and 1 mmol NaCl was added into the solution to form AgCl colloid precipitates And then, ammonia solution (25-28 wt %) was added into the previous colloid solution drop by drop to form clear solution with stirring for several minutes. Subsequently, 0.5 g as-prepared amorphous silica was added into the solution with vigorously stirring for 5 min. The final colloid solution was transformed to 30 mL Teflon lined autoclave and kept at 180 °C for 24h. The final product was centrifuged and washed with absolute alcohol and double-distilled water three times. For comparison, the reaction was conducted at different temperature (eg. 140 °C, 160 °C), while other experimental conditions were kept the same.

3.3 Antibacterial experiments

For antibacterial experiments, the bacterial strains were first cultured on the agar plates. Escherichia Coli (E. Coli) was collected and diluted to a cell density of 1×10^5 $CFU\cdot mL^{-1}$ in complete medium. Every sample was tested three times for statistics data and the results were averaged. The minimal inhibitory concentrations (MICs) and minimum bactericidal concentrations (MBCs), adopted to quantitative analysis the bacteriostatic and bactericidal properties of the samples against different pathogenic organisms, were defined as the endpoint where no visible turbidity could be detected with respect to controls and the lowest concentration of the tested agent that produced no colonies on the plate by 24h, respectively, and determined by a broth dilution method.[42]

Photocatalytic performance of SiO_2/Ag microspheres. The photodecomposition of R6G solution was carried out in a 50 mL beaker containing 10 mL R6G solution (1×10^{-5}M) and 4 mg SiO_2/Ag microspheres, and then 0.4 mL freshly prepared $NaBH_4$ (0.1M) was added. The solution was irradiated under visible light irradiation of a 250 W Xe lamp with a 420 nm cutoff filter. The concentration of Rh6G was measured by UV–vis spectrophotometer (2501 PC model; Shimadzu, Kyoto, Japan) at 2 min interval.

3.4 Characterization. The phase of the as-prepared product was characterized by X-ray power diffraction (XRD) analyses, which was carried out on a Philips X'Pert PRO SUPER X-ray diffractometer equipped with graphite monochromatized Cu Kα radiation and the operation voltage and current were maintained at 40 kV and 40 mA, respectively. The morphology and size of the samples were investigated by field-emission scanning electron microscopy (FESEM, JEOL-6700F) and transmission electron microscopy (TEM, JEOL 3010). The UV-vis spectroscopy was recorded on SHIMADZU UV-2501. The Brunauer-Emmett-Teller (BET) specific surface area of the samples was carried out on Quantachrome Autosorb-1 (Quantachrome, USA) and the samples were degassed in a vacuum at 200 ^{o}C for 2 h.

4. Conclusions

In summary, we have demonstrated that a facile hydrothermal process has been successfully developed to synthesize uniform silica/ultrasmall silver composite microspheres from $[Ag(NH_3)_2]^+$ in presence of silica microspheres. The reaction temperature plays a critical role in the formation of the as-prepared SiO_2/ultrasmall Ag composite microspheres. The silica/ultrasmall silver composite microspheres are with 200 nm in diameters and the silica microspheres decorated with ultrasmall Ag nanoparticles with an average diameter of 4 nm. The as-prepared silica/ultrasmall silver composite microspheres exhibit superior and durable bacteriostatic, bactericidal and photocatalytic activities owing to the antimicrobial ability of the ultrasmall Ag nanoparticles embedded in silica microspheres. The

SiO_2/ultrasmall Ag composite microspheres would be found widely used in wastewater treatment, water and air filtration to eliminate microorganisms.

Acknowledgements

This work was financial supported by the National Science Foundation of China (Grants No. 21101140), Zhejiang Qianjiang Talent Project (2012R10062) and the Fundamental Research Funds for the Central Universities (2013HGXK0022, 2013HGCH0001) and the Zhejiang Provincial Natural Science Foundation of China (Grants No.LQ12C05001). X. H. Liu, Y. Y. Cao and H. Y. Peng contributed equally to this work.

References

Institute of Smart Biomedical Materials and Device, School of Medical Engineering, Hefei University of Technology, Hefei 230009, P. R. China. Fax: 0086 551 62901285, Fax: 0086 551 62901285; E-mail: shqian@hfut.edu.cn (Prof. H.S. Qian), hbzhang@hfut.edu.cn (Prof. H.B. Zhang). Department of Chemistry, College of Chemistry and Life Sciences, Zhejiang Normal University, Jinhua 321004, P. R. China.

---

1 (a) S. E. Skrabalak, J. Y. Chen, Y. G. Sun, X. M. Lu, L. Au, C. M. Cobley and Y. N. Xia, Acc. Chem. Res., 2008, **41**, 1587. (b) C. Sönnichsen, B. M. Reinhard, J. Liphardt and A. P. Alivisatos, Nat. Biotech., 2005, **23**, 741.

2 (a) X. H. Huang, I. H. EI-Sayed, W. Qian and M. A. EI-Sayed, J. Am. Chem. Soc., 2006, **128**, 2115. (b) N. Tian, Z. Y. Zhou, S. G. Sun, Y. Ding and Z. L. Wang, Science, 2007, **316**, 732. (c) D. C. Kennedy, K. A. Hoop, L. L. Tay, J. P. Pezacki, Nanoscale, 2010, **2**, 1413

3 S. E. Skrabalak, L. Au, X. D. Li and Y. N. Xia, Nature Protocols, 2007, **2**, 2182.

4 L. J. Sherry, S. H. Chang, G. C. Schatz, R. P. Van Duyne, B. J. Wiley and Y. N. Xia, Nano Lett., 2005, **5**, 2034.

5 J. Zeng, Y. Q. Zheng, M. Rycenga, J. Tao, Z. Y. Li, Q. Zhang, Y. M. Zhu and Y. N. Xia, J. Am. Chem. Soc., 2010, **132**, 8552.

6 B. Wiley, Y. Sun, B. Mayers and Y. Xia, Chem. -Eur. J., 2005, **11**, 454.

7 Y. Zhou, S. H. Yu, C. Y. Wang, X. G. Li, Y. R. Zhu and Z. Y. Chen, Adv. Mater., 1999, **11**, 850.

8 D. Seo, C. Il Yoo, J. Jung and H. Song, J. Am. Chem. Soc., 2008, **130**, 2940.

9 W. M. Schuette and W. E. Buhro, ACS Nano, 2013, **7**, 3844.

10 W. L. Yang, J. J. Li, Y. J. Zhong, H. S. Qian, Z. Q. Li and Y. Hu, CrystEngComm, 2013, **15**, 2598.

11 C. H. An, S. Peng and Y. G. Sun, Adv. Mater., 2010, **22**, 2570.

12 X. Yuan, M. I. Setyawati, A. S. Tan, C. N. Ong, D. T. Leong and J. P. Xie, NPG Asia Mater., 2013, **5**, e39.

13 H. Y. Lee, H. K. Park, Y. M. Lee, K. Kim and S. B. Park. Chem. Commun., 2007, 2959.

14 D. Maity, M. Kanti Bain, B. Bhowmick, J. Sarkar, S. Saha, K. Acharya, M. Chakraborty and D. J. Chattopadhyay, J. Appl. Polym. Sci., 2011, **122**, 2189.

15 G. A. Martínez-Castañón, N. Niño-Martínez, F. Martínez-Gutierrez, J. R. Martínez-Mendoza and F. Ruiz, J. Nanopart. Res., 2008, **10**, 1343.

16 T. Y. Zhang, X. Q. Li, S. Z. Kang, L. X. Qin, W. F. Yan and J. Mu, J. Colloid Inter. Sci., 2013, **402**, 279.

17 R. Nirmala, D. Kalpana, R. Navamathavan, Y. S. Lee and H. Y. Kim, J. Nanosci. Nanotechnol., 2013, **13**, 4686.

18 Z. J. Jiang, C. Y. Liu and L. W. Sun, J. Phys. Chem. B, 2005, **109**, 1730.

19 S. M. Sun and Y. D. Li, Angew. Chem. Int. Ed., 2004, **43**, 3827

20 B. Hu, Y. Zhao, H. Z. Zhu and S. H. Yu, ACS Nano, 2011, **5**, 3166.

21 Z. W. Deng, H. B. Zhu, B. Peng, H. Chen, Y. F. Sun, X. D. Gang, P. J. Jin and J. L. Wang, ACS Appl. Mater. Interfaces, 2012, **4**, 5625.

22 R. Kumar, S. Howdle and H. Münstedt, J. Biomed. Mater. Res. Part B, 2005, **75B**, 311.

23 M. H. Wang, J. W. Fu, D. D. Huang, C. Zhang, Q. Xu, Nanoscale, 2013, **5**, 7913.

24 C. Liu, D. Yang, Y. Jiao, Y. Tian, Y. G. Wang and Z. Y. Jiang, ACS Appl. Mater. Interfaces, 2013, **5**, 3824.

25 H. B. Hu, Z. H. Wang, L. Pan, S. P. Zhao and S. Y. Zhu, J. Phys. Chem. C, 2010, **114**, 7738.

26 Z. W. Deng, M. Chen and L. M. Wu, J. Phys. Chem. C, 2007, **111**, 11692.

27 J. L. Hu, H. S. Qian, J. J. Li, Y. Hu, Z. Q. Li and S. H. Yu, Part. Part. Syst. Charact., 2013, **30**, 306.

28 J. L. Hu, Q. H. Yang, H. Lin, Y. P. Ye, Q. He, J. N. Zhang and H. S. Qian, Nanoscale, 2013, 5, 6327.

29 Z. Wang, J. Liu, X. Chen, J. Wan and Y. Qian, Chem. -Eur. J., 2004, **11**, 160.

30 H. Lu, H. F. Ju, Q. Yang, Z. R. Li, H. Y. Ren, X. Xin and G. Y. Xu, CrystEngComm, 2013, **15**, 6511.

31 G. Mie, Ann. Phys., 1908, **25**, 377.

32 J. A. Scholl, A. L. Koh and J. A. Dionne, Nature, 2012, **483**, 421.

33 C. Sella, S. Chenot, V. Reillon and S. Berthier, Thin Solid Films, **2009**, 517, 5848.

34 Y. Onodera, T. Iwasaki, A. Chatterjee, T. Ebina, T. Satoh, T. Suzuki, H. Mimura, Appl. Clay Sci.,

2001, **18**, 123.

35 J. S. Hammond, S. W. Gaarenstroom and N. Winograd, Anal. Chem., 1975, **47**, 2194.

36 S. W. Gaarenstroom and N. Winograd, J. Chem. Phys., 1977, **67**, 3500.

37 W. Li, Y. H. Deng, Z. X. Wu, X. F. Qian, J. P. Yang, Y. Wang, D. Gu, F. Zhang, B. Tu and D.Y. Zhao, J. Am. Chem. Soc., 2011, **133**, 15830.

38 Q. Zhang, T.R. Zhang, J.P. Ge and Y.D. Yin, Nano Lett., 2008, **8**, 2867.

39 J. S. Kim, E. Kuk, , K. N.Yu, J. H. Kim, S. J. Park, H. J. Lee, S. H. Kim, Y. K. Park,Y. H. Park, C. Y. Hwang, Y. K. Kim, Y. S. Lee, D. H. Jeong and M. H. Cho, Nanomed. Nanotechnol., 2007, **3**, 95.

40 H. J. Park, J. Y. Kim, J. Kim, J. H. Lee, J. S. Hahn, M. B. Gu and J. Yoon, Water Res., 2007, **43**, 1027.

41 J. A. Scholl, A. L. Koh and J. A. Dionne, Nature, 2012, **483**, 421.

42 M. Fang, J. H. Chen, X. L. Xu, P. H. Yang and H. F. Hildebrand, Int. J. Antimicrob. Ag., 2006, **27**, 513.

Graphic abstract

Silica/Ultrasmall Ag Composite microspheres (see Figure): Uniform silica/ultrasmall silver composite microspheres has been successfully prepared from silica microspheres and $[Ag(NH_3)_2]^+$ via hydrothermal process. The silica microspheres decorated with ultrafine silver nanoparticles with an average size of 4 nm; which exhibit excellent antibacterial performance on E. Coli.